AIAA SciTech Forum
January 3-7, 2022, San Diego, CA & Virtual
AIAA SCITECH 2022 Forum

10.2514/6.2022-1449

2D modeling of the electrode geometry effects on plasma-assisted H_2/air ignition

Xingqian Mao[1], Hongtao Zhong[2] and Yiguang Ju[3]
Princeton University, Princeton, NJ 08544, USA

This work presents the results of two-dimensional modeling of the electrode geometry effects on H_2/air ignition in a nanosecond plasma discharge. A new multi-scale adaptive reduced chemistry solver for plasma assisted combustion (MARCS-PAC) is applied to simulate the effects of electrode shape, diameter and gap size on ignition enhancement. The results show that a cylindrical electrode produces larger ignition kernel compared with spherical and parabolical electrodes by generating a larger discharge volume with active species and gas heating. There exists a non-monotonic dependence of ignition kernel volume on electrode diameter and gap size. This work provides insights to understand the effects of electrode geometry on the optimization of ignition enhancement in advanced engines.

I. Introduction

The advantages of non-equilibrium plasma have drawn great attention in ignition enhancement [1], flammability extension [2], engine performance improvement [3] and low temperature combustion [4] in combustion engines. Volumetric production of active species such as vibrationally and electronically excited species, radicals, ions and electrons, as well as gas heating in a nanosecond discharge can enhance ignition via kinetic, thermal and transport pathways [5]. However, the quantitative understanding of multi-dimensional dynamics of the coupling of localized streamer development and active species as well heat production between plasma discharge and combustion chemistry are still not well-understood.

To understand the physical and chemical processes of plasma assisted combustion, different numerical modeling tools have been developed in recent years, including zero-dimensional (0D) [6, 7], one-dimensional (1D) [8, 9], two-dimensional (2D) [10, 11] and three-dimensional (3D) [12] models. To capture the dynamics of filament discharge development of plasma and ignition kernel development with optimum ignition enhancement in practical engines, a multi-dimensional model considering electrode geometry is needed. For example, the experiments conducted by Lo et al. [13] and Pancheshnyi et al. [14] showed that the flame first appeared near the electrodes and then propagated along the inter-electrode and to the outside space with a point-to-plane discharge geometry in propane/air mixtures. Moreover, the results showed the flame kernel size generation near the electrodes was also affected by the different configurations of the point-to-plane electrodes [13]. The experimental studies of Lefkowitz and Ombrello [15, 16] showed that the electrode gap size affected the effective ignition kernel development. These studies indicate that different configurations of electrode geometry play an important role in the optimization of ignition enhancement. Therefore, further studies of the effects of electrode geometry on discharge dynamics and ignition are of interest.

Recently, the authors developed a two-dimensional multi-scale adaptive reduced chemistry solver for plasma assisted combustion (MARCS-PAC) [17]. The model integrates the 2D plasma solver PASSKEy [18-21] and the adaptive simulation of unsteady reactive 2D flow solver ASURF+ [22-24], which provides a 2D computational platform for the multi-dimensional modeling of plasma assisted combustion with detailed chemistry and transport.

The objective of this work is to study the effects of electrode geometry on plasma assisted H_2/air ignition. Firstly, the ignition kernel development in a nanosecond discharge with different electrode geometry is studied. Then, the effects of electrode shape, electrode diameter and electrode gap size on ignition are investigated. Finally, the optimum electrode geometry for plasma assisted ignition is discussed.

---

[1] Postdoctoral Research Associate, Department of Mechanical and Aerospace Engineering, xingqian@princeton.edu.
[2] Ph.D. Candidate, Department of Mechanical and Aerospace Engineering, AIAA Student Member.
[3] Robert Porter Patterson Professor, Department of Mechanical and Aerospace Engineering, AIAA Associate Fellow.

II. Numerical methods

The governing equations of the MARCS-PAC model are briefly described as below.

The continuity equation for electrons, ions, excited species, intermediate species, reactants and products in plasma is

$$\frac{\partial n_k}{\partial t} + \vec{\nabla}\cdot\vec{J_k} = S_k + S_{\mathrm{ph}} \tag{1}$$

where n_k is the number density of species k, t the time, $\vec{J_k}$ the flux vector of species k due to drift-diffusion of charged species with electric field, and S_k and S_{ph} the production or consumption rate of species k contributed by plasma kinetics and photoionization, respectively.

The flux vector $\vec{J_k}$ is calculated by the drift-diffusion approximation,

$$\vec{J_k} = z_k \mu_k n_k \vec{E} - D_k \vec{\nabla} n_k \tag{2}$$

where z_k is the charge number of species k, μ_k and D_k the mobility and the diffusion coefficient of charged species, respectively, and $\vec{E}$ the electric field vector.

The electric potential is solved by Poisson's equation,

$$\vec{\nabla}\cdot(-\varepsilon_0 \varepsilon \vec{\nabla}\varphi) = \mathrm{q_e} \sum_k z_k n_k \tag{3}$$

where ε_0 is the permittivity of free space, ε the relative dielectric constant, φ the electric potential ($\vec{E} = -\vec{\nabla}\varphi$), and $\mathrm{q_e}$ the absolute value of electron charge.

The discharge solution from PASSKEy [18-21] is coupled with the unsteady, multi-component, reactive, compressible Navier-Stokes (N-S) reactive 2D flow solver ASURF+ [22-24]. The two-dimensional axisymmetric conservation equations of mass, momentum and energy are listed as follows,

$$\frac{\partial \rho}{\partial t} + \vec{\nabla}\cdot(\rho\vec{V}) = 0 \tag{4}$$

$$\frac{\partial(\rho\vec{V})}{\partial t} + \vec{\nabla}\cdot(\rho\vec{V}\vec{V}) = -\vec{\nabla}p + \vec{\nabla}\cdot\bar{\bar{\tau}} \tag{5}$$

$$\frac{\partial e}{\partial t} + \vec{\nabla}\cdot((e+p)\vec{V}) = -\vec{\nabla}\cdot\vec{q} + \vec{\nabla}\cdot(\bar{\bar{\tau}}\vec{V}) + P_{\mathrm{gas}} \tag{6}$$

where ρ is the gas mass density, $\vec{V}$ the velocity vector, p the pressure, $\bar{\bar{\tau}}$ the viscous stress tensor, e the total energy per unit volume, and $\vec{q}$ the heat flux vector. The gas heating P_{gas} from plasma is a source term of Eq. (6).

The conservation equation of species k consisting both plasma and combustion kinetics is given as,

$$\frac{\partial(\rho Y_k)}{\partial t} + \vec{\nabla}\cdot[\rho(\vec{V}+\vec{V_k'})Y_k] = \omega_k \tag{7}$$

$$\omega_k = \omega_k^{\mathrm{plasma}} + \omega_k^{\mathrm{combustion}} \tag{8}$$

$$\omega_k^{\mathrm{plasma}} = S_k + S_{\mathrm{ph}} - \vec{\nabla}\cdot\vec{J_k} \tag{9}$$

where Y_k and $\vec{V_k'}$ are the mass fraction and the diffusion velocity of species k, respectively, and ω_k is the production or consumption rate of species k contributed, respectively, by plasma discharge $\omega_k^{\mathrm{plasma}}$ and combustion kinetics $\omega_k^{\mathrm{combustion}}$.

The plasma assisted $H_2/O_2/N_2$ combustion mechanism used in this work consisting of a plasma sub-model and a combustion sub-model. The model is developed and modified based on our previous study [25]. The mechanism consists of 35 species, 68 reactions in the plasma sub-model and 81 reactions in the combustion sub-model. The plasma sub-mech consists of the reactions involving vibrationally excited species $H_2(v1)$, $O_2(v1)$ and $N_2(v1)$, electronically excited species $O_2(a^1\Delta_g)$, $O_2(b^1\Sigma_g^+)$, $O(^1D)$, $N_2(A)$, $N_2(B)$, $N_2(a')$, $N_2(C)$ and $N(^2D)$, ions H_2^+, O_2^+, N_2^+, N_4^+, O^- and O_2^- as well as electrons. The electron impact vibrational, electronic, dissociation, ionization and attachment, as well as quenching of vibrationally and electronically excited species, charge exchange, electron detachment, ion-ion and electron-ion recombination reactions are included in the plasma sub-model. A detailed $H_2/O_2/N_2$ combustion mechanism from HP-Mech [26] with NO_x formation [27, 28] and O_3 sub-mechanisms [29] are used.

All the calculations were conducted in a stoichiometric H_2/air mixture at 800 K and atmospheric pressure. A single nanosecond discharge pulse was used. A trapezoidal waveform voltage with a rise time of 2 ns and a peak voltage of 2000-5000 V was applied to the electrodes. For the comparison of the effects of different electrode geometries on plasma assisted ignition, the same deposited energy of 0.4 mJ was set for all simulations. The end time of nanosecond discharge is controlled by the discharge energy. The system is assumed to be adiabatic.

For the study of the effects of electrode shape, three types of cylindrical, spherical and parabolical were compared. The length of parabolical or spherical parts of electrodes was 1 mm and the rest part of electrode remained cylindrical with a diameter of 2 mm. The minimum gap size was 2 mm. For the study of the effects of electrode diameter on plasma assisted ignition, the cylindrical electrodes with a gap size of 2 mm was used. The electrode diameter was varied from 1.0 to 2.0 mm. The effects of electrode gap size were studied by using the cylindrical electrodes with a diameter of 2 mm. The gap size was varied from 0.6 to 2.0 mm.

Due to the axisymmetric electrode geometries studied in this work, the cylindrical coordinates (R, Z) are used for all modeling. R-axis indicates the direction of electrode radius and Z-axis indicates the direction of electrode length. The computational domain used in the simulation was 5×10 mm^2. A fine and uniform square mesh was used in the plasma discharge and ignition kernel propagation region with the mesh size of 10 μm × 10 μm, and the mesh size increases exponentially up to the rest of the computational domain.

III. Results and discussion

Fig. 1 shows the time evolutions of temperature during plasma assisted H_2/air ignition with cylindrical, spherical and parabolical electrodes at 5000 V. Fig. 1(a) shows that the ignition kernel is firstly formed near the edges of cylindrical electrodes. This is due to the highest electric field and streamer are first generated near the edges of the electrodes because of the local electric field enhancement. The high concentrations of excited species and radicals as well as the fast temperature rise in this region with high energy discharge density accelerate the ignition. Then the ignition kernel propagates into the unburned gas regions. A large volume of high-temperature burned gas is gradually formed at t = 90 μs. However, compared with the wide discharge channel between the cylindrical electrodes, a very narrow discharge channel is formed for the spherical and parabolical electrodes. Therefore, small ignition kernels are quickly formed at the tips of anode and cathode, as shown in Fig. 1 (b) and (c) at t = 1 μs. After that, the ignition kernel propagates to the unburned gas region from these hot spots. It is noted that the initial ignition kernels are formed faster with spherical and parabolical electrodes, however, the final ignition kernel volumes at t = 90 μs are smaller than that of cylindrical electrodes.

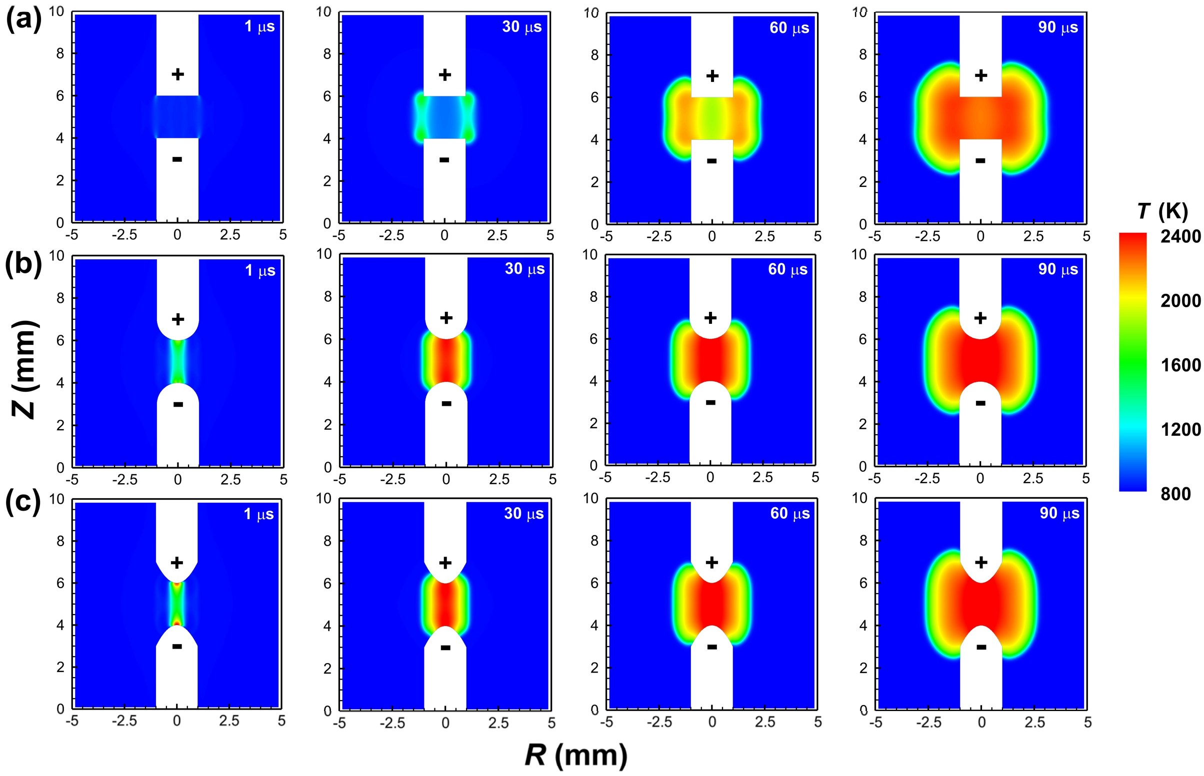

Fig. 1 Time evolutions of temperature during plasma assisted H_2/air ignition with (a) cylindrical, (b) spherical and (c) parabolical electrodes at 5000 V.

Fig. 2 shows the time evolutions of ignition kernel volume with different electrode shapes. The ignition volume is obtained by integrating the volume when the temperature is above 1200 K. The results show that the initial flame kernel formation with spherical and parabolical electrodes is faster than cylindrical electrodes below 30 μs. This fast ignition is because higher active species concentrations and temperature are produced near the axis of discharge gap with higher energy density in the discharge channel. It can be seen that the growth of ignition kernel with cylindrical electrodes exceeds the cases of spherical and parabolical electrodes after 40 μs. This can be explained by smaller peak concentration of active species and smaller temperature increase, but much larger discharge volume produced with cylindrical electrodes. The above analysis indicates that a larger discharge volume with active species production in discharge plays an important role in the ignition enhancement.

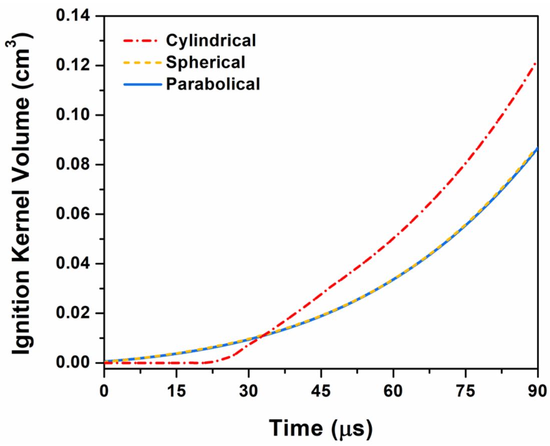

Fig. 2 Time evolutions of ignition kernel with different electrode shapes at 5000 V.

To study the effects of electrode diameter on plasma assisted H_2/air ignition, the ignition kernel volume at t = 90 μs is compared at different electrode diameters, as shown in Fig. 3. The applied voltage was 5000 V. The results show that the maximum ignition kernel volume was reached with the electrode diameter of 1.8 mm. The active species concentrations and gas temperature rise in the discharge channel increase with smaller electrode diameters. However, the smaller discharge volume decelerates the ignition development. In the case of electrode diameter of 2.0 mm, even a larger discharge volume is generated, the ignition kernel volume decreases because of the lower active species concentrations and smaller temperature increase produced in plasma. Therefore, there exists an optimum electrode diameter to achieve the maximum ignition enhancement.

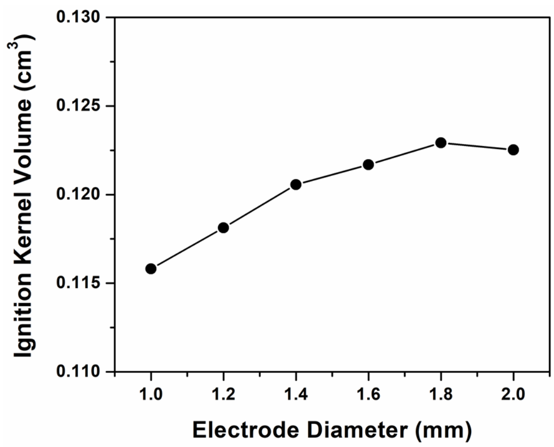

Fig. 3 Ignition kernel volume in plasma assisted H_2/air ignition with different electrode diameters at 5000 V.

Fig. 4 shows the ignition kernel volume at t = 90 μs with different electrode gap sizes at 2000 V. The results show that the ignition kernel volume firstly increases with the decrease of electrode gap size. The maximum ignition kernel volume is reached at the condition with electrode gap size of 0.8 mm. The further decrease of electrode gap size decreases the ignition kernel volume. Previous discussion shows that the ignition development is affected by both the discharge volume and species concentrations produced by plasma. The decrease of electrode gap size results in more discharge energy deposited into a smaller volume and an increase of active species concentrations in the gap. Meanwhile, the decrease of electrode gap size also increases the reduced electric field strength E/N (where N is the gas number density) and therefore species production. The increase of E/N at smaller gap sizes promotes the production of electronically excited species and radicals, further enhancing ignition kinetically [1]. When the gap size is smaller than 0.8 mm, the decrease of discharge volume becomes the domain factor which decreases the ignition development.

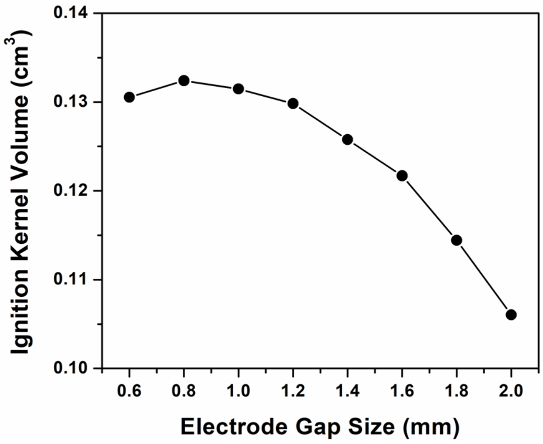

Fig. 4 Ignition kernel volume in plasma assisted H_2/air ignition with different gap sizes at 2000 V.

IV. Conclusion

This work studied the effects of electrode geometries on H_2/air ignition in a nanosecond plasma discharge by 2D modeling. The 2D multi-scale adaptive reduced chemistry solver for plasma assisted combustion (MARCS-PAC) based on PASSKEy discharge modeling package and compressible multi-component reactive flow solver ASURF+ was applied to study the effects of electrode shape, diameter and gap size on plasma assisted H_2/air ignition. The results showed that the plasma assisted ignition is significantly affected by the electrode geometry due to the redistribution of plasma density and electric field. A larger ignition kernel volume formed with the cylindrical electrodes compared with spherical and parabolical electrodes indicated that a larger discharge volume with active species production plays an important role in enhancing ignition. It was shown that there exists the optimum electrode geometry reaching the maximum ignition enhancement with the same discharge energy.

Acknowledgments

This work was partly supported by the grants of DOE Plasma Science Center (DE-SC0020233) and National Science Foundation (CBET-1903362 and NSF-EFRI CBET-2029425). The authors would like to thank the great help of the young research group at Atelier des Plasmas in implementing the PASSKEy solver.

References

[1] Starikovskiy, A., and Aleksandrov, N., "Plasma-assisted ignition and combustion," *Progress in Energy and Combustion Science*, Vol. 39, 2013, pp. 61-110.

[2] Choe, J., Sun, W., Ombrello, T., and Carter, C., "Plasma assisted ammonia combustion: Simultaneous NOx reduction and flame enhancement," *Combustion and Flame*, Vol. 228, 2021, pp. 430-432.

[3] Starikovskiy, A., Aleksandrov, N., and Rakitin, A., "Plasma-Assisted Ignition and Deflagration-to-Detonation Transition," *Philosophical Transactions of the Royal Society A*, Vol. 370, 2012, pp. 740-773.

[4] Ju, Y., Lefkowitz, J. K., Reuter, C. B., Won, S. H., Yang, X., Yang, S., Sun, W., Jiang, Z., and Chen, Q., "Plasma Assisted Low Temperature Combustion," *Plasma Chemistry and Plasma Processing*, Vol. 36, No. 1, 2016, pp. 85-105.

[5] Ju, Y., and Sun, W., "Plasma assisted combustion: Dynamics and chemistry," *Progress in Energy and Combustion Science,* Vol. 48, 2015, pp. 21-83.

[6] Mao, X., Chen, Q., Rousso, A. C., Chen, T. Y., and Ju, Y., "Effects of controlled non-equilibrium excitation on $H_2/O_2/He$ ignition using a hybrid repetitive nanosecond and DC discharge," *Combustion and Flame*, Vol. 206, 2019, pp. 522–535.

[7] Zhong, H., Mao, X., Rousso, A. C., Patrick, C. L., Yan, C., Xu, W., Chen, Q., Wysocki G., and Ju, Y., "Kinetic study of plasma-assisted n-dodecane/O_2/N_2 pyrolysis and oxidation in a nanosecond-pulsed discharge," *Proceedings of the Combustion Institute*, Vol. 38, 2021, pp. 6521-6531.

[8] Yang, S., Nagaraja, S., Sun, W., and Yang, V., “Multiscale modeling and general theory of non-equilibrium plasma-assisted ignition and combustion,” *Journal of Physics D: Applied Physics*, Vol. 50, 2017, 433001.
[9] Zhong, H., Shneider, M. N., Mokrov, M. S., and Ju, Y., “Thermal-chemical instability of weakly ionized plasma in a reactive flow,” *Journal of Physics D: Applied Physics*, Vol. 52, 2019, 484001.
[10] Kobayashi, S., Bonaventura, Z., Tholin, F., Popov N. A., and Bourdon, A., “Study of nanosecond discharges in H_2–air mixtures at atmospheric pressure for plasma assisted combustion applications,” *Plasma Sources Science and Technology*, Vol. 26, 2017, 075004.
[11] Castela, M., Fiorina, B., Coussement, A., Gicquel, O., Darabiha, N., and Laux, C. O., “Modelling the impact of non-equilibrium discharges on reactive mixtures for simulations of plasma-assisted ignition in turbulent flows,” *Combustion and Flame*, Vol. 166, 2016, pp. 133-147.
[12] Castela, M., Stepanyan, S., Fiorina, B., Coussement, A., Gicquel, O., Darabiha, N., and Laux, C. O., “A 3-D DNS and experimental study of the effect of the recirculating flow pattern inside a reactive kernel produced by nanosecond plasma discharges in a methane-air mixture,” *Proceedings of the Combustion Institute*, Vol. 36, 2017, pp. 4095-4103.
[13] Lo, A., Frat, F., Domingues, E., Lacour, A., Lecordier, B., Vervisch, P., and Cessou, A., “Nanosecond pulsed discharge in a propane–air mixture: Ignition and energy deposition,” *Proceedings of the Combustion Institute*, Vol. 36, 2017, pp. 4087-4094.
[14] Pancheshnyi, S. V., Lacoste, D. A., Bourdon, A., and Laux, C. O., “Ignition of propane–air mixtures by a repetitively pulsed nanosecond discharge,” *IEEE Transactions on Plasma Science*, Vol. 34, 2006, pp. 2478-2487.
[15] Lefkowitz, J. K., and Ombrello, T., “An exploration of inter-pulse coupling in nanosecond pulsed high frequency discharge ignition,” *Combustion and Flame*, Vol. 180, 2017, pp. 136–147.
[16] Lefkowitz, J. K., and Ombrello, T., “Reduction of flame development time in nanosecond pulsed high frequency discharge ignition of flowing mixtures,” *Combustion and Flame*, Vol. 193, 2018, pp. 471–480.
[17] Mao, X., Zhong, H., and Y. Ju, “2D modeling of plasma-assisted H_2/air ignition in a nanosecond discharge with detailed chemistry,” *AIAA Scitech 2021 Forum*, 2021, AIAA 2021-1790.
[18] Zhu, Y., Chen, X., Wu, Y., and Starikovskaia, S., PASSKEy code [software]. Available from http://www.plasma-tech.net/parser/passkey/ (Science and Technology of Plasma Dynamics Laboratory, Xi’an, China and Laboratoire de Physique des Plasmas, Paris, France, 2021).
[19] Chen, X., Zhu, Y., and Wu, Y., “Modeling of streamer-to-spark transitions in the first pulse and the post discharge stage,” *Plasma Sources Science Technology*, Vol. 29, 2020, 095006.
[20] Zhu, Y., Shcherbanev, S., Baron, B., and Starikovskaia, S., “Nanosecond surface dielectric barrier discharge in atmospheric pressure air: I. measurements and 2D modeling of morphology, propagation and hydrodynamic perturbations,” *Plasma Sources Science Technology*, Vol. 26, 2017, 125004.
[21] Chen, X., Zhu, Y., Wu, Y., Hao, J., Ma, X., and Lu, P., “Modeling of fast ionization waves in pure nitrogen at moderate pressure,” *Plasma Sources Science Technology*, Vol. 30, 2021, 065002.
[22] Chen, Z., “Studies on the initiation, propagation, and extinction of premixed flames,” Ph.D. Dissertation, The Dept. of Mechanical and Aerospace Engineering, Princeton University, Princeton, NJ, 2009.
[23] Chen, Z., Burke, M. P., and Ju, Y., “Effects of Lewis number and ignition energy on the determination of laminar flame speed using propagating spherical flames,” *Proceedings of the Combustion Institute*, Vol. 32, 2009, 1253-1260
[24] Sun, W., “Developments of Efficient Numerical Methods for Combustion Modeling with Detailed Chemical Kinetics,” Ph.D. Dissertation, The Dept. of Mechanical and Aerospace Engineering, Princeton University, Princeton, NJ, 2020.
[25] Zhong, H., Shneider, M. N., Mao, X., and Ju, Y., “Dynamics and chemical mode analysis of plasma thermal-chemical instability,” *Plasma Sources Science Technology*, Vol. 30, 2021, 035002.
[26] Yang, X., Shen, X., Santner, J., Zhao, H., and Ju Y., Princeton HP-Mech. http://engine.princeton.edu/mechanism/HP-Mech.html, 2017.
[27] Zhao, H., Wu, L., Patrick, C., Zhang, Z., Rezgui, Y., Yang, X., Wysocki, G., and Ju, Y., “Studies of low temperature oxidation of n-pentane with nitric oxide addition in a jet stirred reactor,” *Combustion and Flame*, Vol. 197, 2018, pp. 78–87.
[28] Gokulakrishnan, P., Fuller, C. C., and Klassen, M. S., “Experimental and modeling study of C1–C3 hydrocarbon ignition in the presence of nitric oxide,” *Journal of Engineering for Gas Turbines and Power*, Vol. 140, No. 4, 2018, 041509.
[29] Zhao, H., Yang, X., and Ju, Y., “Kinetic studies of ozone assisted low temperature oxidation of dimethyl ether in a flow reactor using molecular-beam mass spectrometry,” *Combustion and Flame*, Vol. 173, 2016, pp. 187-194.